Application of Compliant control in Pin-Based Shape Display for Compliant Physical Interaction between Human and Machine

Yizhou Huang, Songjie Xiao, Yunze Shi, Haoyu Li and Liangjing Yang, *Senior Member, IEEE*

***Abstract*—Compliant control is widely used in the human-robot interaction (HRI) field. However, very few research pays attention on applying compliant control to the pin-based shaped display which is a type of HRI device widely researched as tangible user interface for the enhancement of the HRI quality. Admittance control as one of the compliant controls is performing well under soft environment which is ideal as a candidate control method for pin-based shape display for the reason that the human body surface is generally soft. In this paper, a pin-based shape display with admittance control will be prototyped. The general control scheme as well as the design methodology will be explained and evaluated. A variable compliant control will be proposed and simulated to achieve even normal force distribution on its surface. Different compliant control parameters will be chosen to evaluate the device under experiment.**

I. Introduction

Shape Displays or Shape Changing Interfaces is a growing research field of HRI over the past decades. These devices can enable tangible and haptic interactions via shape changing [1]. Pin-based shape displays are one of the most representative options among various types of shape displays and its development can be traced back decades ago [2].

Most of the related works are dedicated with interaction related with geometrical sensation. In [3], three pin-based display motion control methods coupled with VR virtual image illusions were proposed to generate visuo-haptic illusions. Such approach creates the illusion of enhanced resolution and pin actuation speed without needing to change the actual hardware of pin-based shape display. In [4], pin-based shape display is mounted on a mobile platform which makes it possible for passively or actively moving the display to make the interaction more lively. In [5], the concept of dynamic physical affordances enable not only the potential interactions between pin-based shape display and human but also the actuation of the objects on the display according to the need of human. In order to improve the resolution and versatility of pin-based shape display, a series of specially designed docks [6] can be easily mounted on the pin-based display.

Some clever designs include using Bowden Cables as motion translation mechanism [5] to reduce distances between pins and configurating the mechanism to reduce the number of motors required [7]. The idea of pin-based shape display can be further extended into bigger scale and served as a large room scaled furniture which enables a novel housing style [8]. Apart from motion, pin-based shape display with direct force control [9] is able to regulate the force interaction between human and shape display. This work enhances the interaction into a different level and widens the application scenarios for shape display.

Most of the researches of pin-based shape display are related with the motion control methods of pin-based shape display and optimizations of the performance of pin-based shape display via clever motion control strategies. Force interaction between human and pin-based shape display as well as the interaction between environment and pin-based shape display are not adequate. Almost no research about pin-based shape display considers the dynamic relation between the motion of pins and interaction force.

Compliant control, including both admittance control and impedance control, enables adjustment of the dynamic properties and interactive behavior of the mechanisms readily within certain limits [10].The qualitative performance of both admittance control and impedance control is illustrated in Figure 1. The qualitative performance comprises both accuracy of dynamical behavior and stability of interaction under different environment stiffness. The admittance control is performing with better accuracy of dynamical behavior under soft environment, but will have stability issue under stiff environment. The impedance control is vice versa. In this paper, admittance control is chosen as the candidate control method for it performs better under soft interaction.

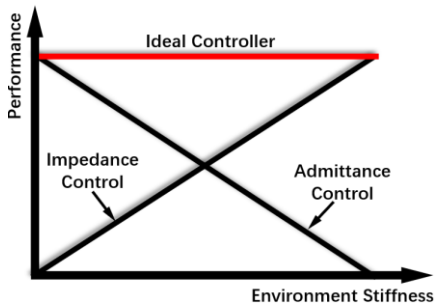

Figure 1. Illustrations of performance between two different controls under different stiffness [11]

The overall structure of the pin-based shape display system is shown as the Figure 2. The sensing part senses contact force between human and pin-based shape display. Then after embedded system processing the data acquired from sensing part and completing computation of the motion command under the law of admittance control, the linear actuator conducts certain motion under motion control of embedded

This work was supported in part by the International Campus of Zhejiang University (iZJU) "Human Space X" Initiative Phase I: Tiantong Multidisciplinary Seed Grant, led by Principal Supervisor Liangjing Yang.
Yizhou Huang and Haoyu Li are graduate students at Zhejiang University/University of Illinois at Urbana-Champaign Institute, Zhejiang University, Haining, China, Songjie Xiao and Yunze Shi are Ph.D. students at Zhejiang University.

system. The compliant interaction between human and pin-based shape display is realized. The development interface enables intuitive status monitoring of the system as well as adjustments of the admittance parameters.

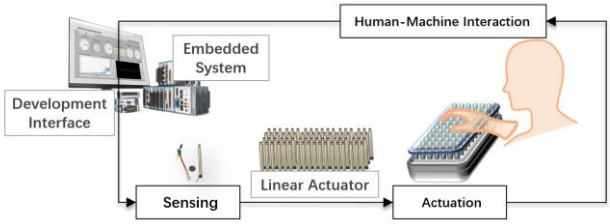

Figure 2. Overall structure of the system

A 4-by-4 pin-based shape display with compliant control is proposed in this paper. The paper will be organized as the follows. The methodology of both admittance control with fixed and variable compliant control parameters will be explained at first. Admittance control with variable compliant control parameters will then be evaluated under simulation. The general structure of the prototype is then explained. The experiments for evaluation are conducted afterwards and results are provided. Lastly, future applications and research will be discussed.

II. ADMITTANCE CONTROL SCHEMES

A. Pin-based shape display admittance controller with fixed compliant control parameters

The general structure of Pin-based shape display with fixed compliant control parameters is shown in Figure 3. First, consider the device is operated passively which means the device will not move without external force applied on it. Position and velocity at equilibrium position X0 without external force applied on the pin is set to be zero. The desired position x_d is generated by the following equation:

$$-F_{ext} = K_d(x_d - \mathrm{X0}) \tag{1}$$

Where F_{ext} is the magnitude of external force applied on each pin which is measured by thin film pressure sensor and K_d is the designed fixed stiffness parameter of this admittance controller.

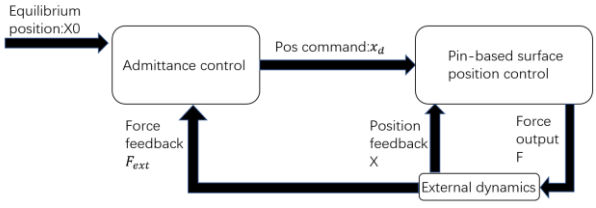

Figure 3. Proposed admittance control scheme with fixed compliant parameter

If the target position of a pin is above the current position X the velocity command $\dot{x}_d$ to pin is upward and vice versa. The velocity command is generated by the following equation:

$$\dot{x}_d = \frac{K_d(x_d - X)}{D_d} \tag{2}$$

where D_d is the designed fixed parameter to mimic damping effect.

$$-F_{ext} = K_d\, X + D_d\dot{x}_d \approx K_d\, X + D_d\dot{X} \tag{3}$$

Assuming the response of motor so well that $\dot{x}_d$ can be seen as same as $\dot{X}$. Then the pin shows some spring-damping like property. Also, the damping of compression (pin goes down) and rebound (pin goes up) can be set separately. For simplicity, we eliminated the inertia term. What's more damping term is more noticeable for human than inertia term [12]. The position controller can be implemented as PD controller [11] which can be written as:

$$F = k_p(x_d - X) + k_d\dot{X} \approx k_p(x_d - X) + k_d\dot{x}_d \tag{4}$$

Can be then written as:

$$\begin{aligned} F &\approx k_p(x_d - X) + k_d\dot{x}_d \\ &= \left(k_p\frac{D_d}{K_d} + k_d\right)\dot{x}_d = K\dot{x}_d \end{aligned} \tag{5}$$

where k_p and k_d are the control parameters for PD controller above.

The stability of this control scheme is being discussed as the following. Assuming a mass is interacting with the environment:

$$I_m\ddot{X} = F + F_{ext} \tag{6}$$

Where I_m is the inertia of the pin. Because the motor is moving linearly, the acceleration and velocity of pins are written as $\ddot{X}$ and $\dot{X}$. Combing equation (3), (5) and (6), the transfer function between x_d and X can be written as:

$$\frac{X(S)}{x_d(S)} = \frac{KS}{I_m S^2 + D_d S + K_d} \tag{7}$$

As long as ${D_d}^2 - 4I_mK_d \geq 0$, there is no positive pole, the system is stable.

However, if the motor requires a long time to accelerate to the desired velocity, then the equation (4) will not be valid. There will exist poles on virtual axis, then oscillation may occur. If the ideal assumption of equation (3) is not feasible, then may refer to more conventional approach as following.

$$-F_{ext} = K_d(x_d - 0) + D_d(\dot{x}_d - 0) \tag{8}$$

The equation is the equation of admittance controller, where D_d is the designed damping parameter.

$$\dot{x}_d(t) = \frac{[-F_{ext}(t) - K_dX(t-\Delta t)]}{D_d} \tag{9}$$

To generate desired velocity $\dot{x}_d$ by using the currently measured force input $F_{ext}(t)$ and the latest actual position feedback $X(t-\Delta t)$.

$$x_d(t) = X(t-\Delta t) + \dot{x}_d(t)\Delta t \tag{10}$$

After generating the desired position, then sending $\dot{x}_d(t)$ and $x_d(t)$ into a PD controller to control the output motion:

$$F(t) = k_p(x_d(t) - X(t-\Delta t)) + k_d(\dot{x}_d(t) - \dot{X}(t-\Delta t)) \tag{11}$$

Since the motor used in this device is moving slowly and will not using a long time to get to desired speed. Thus, the simplified approach is feasible.

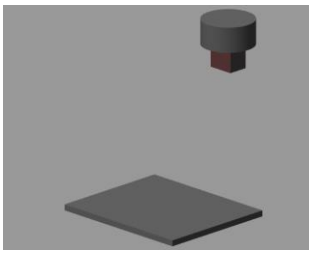

Figure 4. Simulation validation of single pin

Using Simulink to examine the control scheme of the pin can exhibit the spring and damping properties so that it can regulate the relation between external force and motion dynamically. A cylindrical solid weight is 0.5Kg with radius of 22mm and height of 42mm. The top surface of pin is rectangular of 22mm by 17mm with travel of 25mm. k_p and k_d in equation (5) are set to be 1. The stiffness and damping are set to be 420N/m and 400Ns/m correspondingly. The setup of simulation is shown in the Figure 4. The cylindrical solid in simulation is released freely from a position where the centroid of bottom plane of this cylindrical solid is 1mm above the centroid of top surface of pin.

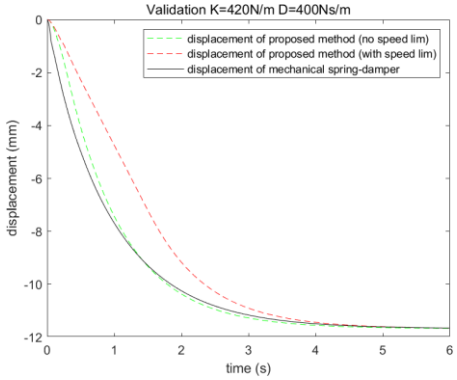

Figure 5. Position with respect to time of the single pin

In Figure 5, where the green dashed line, the red dashed line and the black line are representing the displacement of proposed method without speed limit, the displacement of proposed method with speed limit of 8mm/s and the displace of mechanical spring-damper correspondingly. Their final positions are all -11.68mm which is expected under hooks' law. The green dashed line is quite close to the black line and their correlation coefficient is 0.9984. This means the proposed control scheme is performing very close to the mechanical reference with the same stiffness and damping. Despite the red line shows some form of critical damping property, it deviates a bit from the mechanical reference due to the speed limit. Due to the device is in contact with human, set the speed limit to avoid injury is necessary. In the early real demo of shape display with top speed of 8mm/s is generally safe in practice. However, the balance between top speed of pin for more realistic feeling and safety needs further exploration in future research.

Despite the drawback of top speed making the pin not perform dynamically accurate, the position of single pin with respect to time is similar to that of a critical damping system which means this control scheme can be applied to enable the shape display to mimic properties of mechanical spring-damper to some extent.

B. Pin-based shape display admittance controller with variable compliant control parameters

In this case the D_d will be chosen according to the specification of hardware and a suitable D_d parameter will be fixed. The K_d will be the parameter that is variable according the force distribution among all 16 pins. The general control scheme of Pin-based shape display with variable compliant control parameters is shown in Figure 6.

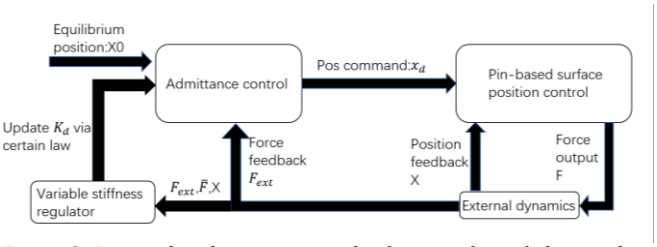

Figure 6. Proposed admittance control scheme with varibale compliant parameter

The scheme inside variable stiffness regulator is shown in the Figure 7.

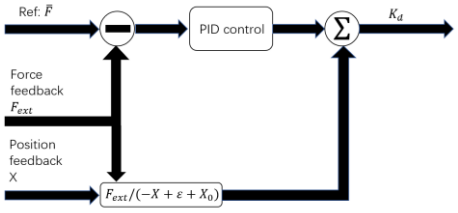

Figure 7. Proposed variable stiffness regulator

K_d is defined as:

$$K_d(S) = \frac{F_{ext}(S)}{-X(S)} + (P + \frac{I}{S} + DS)(\bar{F}(S) - F_{ext}(S)) \quad (12)$$

Where ε is a constant close to zero preventing the K_d from invalid at the point when the pin is at zero position while not letting the pin drift too much from zero position. In here the ε is set to be 10e-6. If we combine equation (1) and (12), and set X0=0:

$$-F_{ext}(S) = \left[\frac{F_{ext}(S)}{-X(S)} + (P + \frac{I}{S} + DS)(\bar{F}(S) - F_{ext}(S))\right] x_d(S) \quad (13)$$

Where P, I and D are the control parameters for PID controller above.

When pins are close to a configuration such that minimize the absolute value of $\bar{F} - F_{ext}$, we assume the $\ddot{X} \approx 0$, the position $X < 0$ and $X0 > 0$, this setup is to avoid $X - X0 = 0$, and as a result:

$$F \approx -F_{ext} = K_d\,(X - X0) + d_d\dot{x}_d \approx K_d\,(X - X0) + d_d\dot{X} \quad (14)$$

When absolute value of $\bar{F} - F_{ext}$ is close to zero, the $K_d \approx \frac{F_{ext}}{-X+X0}$,which means:

$$\begin{aligned} &-F_{ext} \\ &= K_d\,(X - X0) + d_d\dot{x}_d \\ &= \frac{F_{ext}}{-X+X0}(X - X0) + d_d\dot{x}_d \end{aligned} \quad (15)$$

Thus, we can infer that under this condition the $\dot{x}_d = 0$. This means the movement of pins will stop when absolute value of $\bar{F} - F_{ext}$ is close to zero.

K_d must be limited no bigger than $\frac{\max(F_{ext})}{P}$ and no smaller than $\frac{\min(F_{ext})}{P}$. $\max(F_{ext})$ and $\min(F_{ext})$ are determined by the measuring range of the chosen force sensor, P is the travel of pin. When $F_{ext} = \bar{F} = F_{min}$, meaning that there is nothing on the shape display the pin will back to zero position. Also, when the pin is at the maximum travel, it will back to zero position gradually. To evaluate whether this method is functional, a simulation will be conducted in next chapter.

III. Evaluation of Variable Stiffness Control

The setup is a module of 16 pins. A ball with radius of 8cm and weight of 10Kg will be released freely from 6cm above the centroid of the module. According to the specification of our hardware, which will be fully described in next chapter, the top surface of pin is rectangular of 22mm by 17mm with travel of 25mm, distances between each pin are 20.5mm in x direction and 27.5mm in y direction. The range of force sensor is between 0.294N and 14N. the speed of pins are limited within 8mm/s.

$$\frac{F_{min}}{V_{max}} < D \quad (16)$$

The damping we chosen is 400Ns/m. Even this K_d is variable, the value of K_d is also being limited according to the range of force sensor and the traveling range of the pin.

$$11.76N/m = \frac{\min(F_{ext})}{P} < K_d < \frac{\max(F_{ext})}{P} = 560N/m \quad (17)$$

The arrangement of pins and the ball and serial number of pins are shown as the following Figure 8.

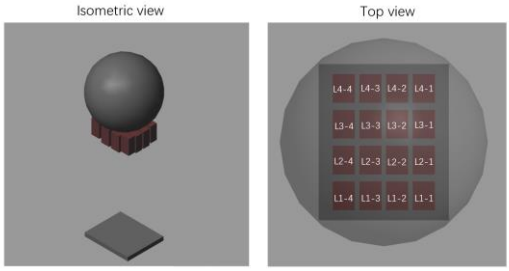

Figure 8. Arrangement of pins and the ball

A. Simulation results and discussions

The standard deviation of forces applied on pins and the time cost of the standard deviation under 1N are chosen as parameters of control scheme evaluation. The bigger the standard deviation the more uneven the force distribution is.

Due to the resolution of this shape display is limited, the standard deviation of force will not reach zero bit only a small value. A threshold must be set to avoid losing control resulted from bottoming up of some pins. The K_d will stop adjusting as the magnitude of standard deviation of force reaches below 10 percent of the average force applied on the entire display. The K_d will resume adjusting once the magnitude of standard deviation of force has exceed that threshold. Also, when the pin is at the maximum stroke the pin will move up to zero position and repeat the adjustment procedure.

The standard deviation of forces applied on pins with respect to time is shown in Figure 9. The elapse time of this simulation is 30s. K_d is adjusted automatically. The standard deviation of force oscillates until 8.10s and then it decreases slowly. The oscillation is mainly due to the ball is a convex shape and the surface of module is comprised of flat planes, plus the deformation of shape display is not instantly. The minimum standard deviation of force is about 0.56N at 20.19s and peak is 11.07N at 1.93s. The time cost of the standard deviation under 1N is 13.02s.

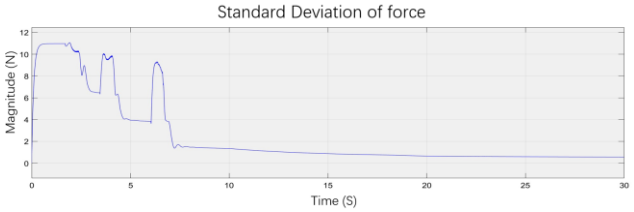

Figure 9. Standard deviation of force with respect to time

Plots of variable stiffness on different pins with respect to time are shown in Figure 10.

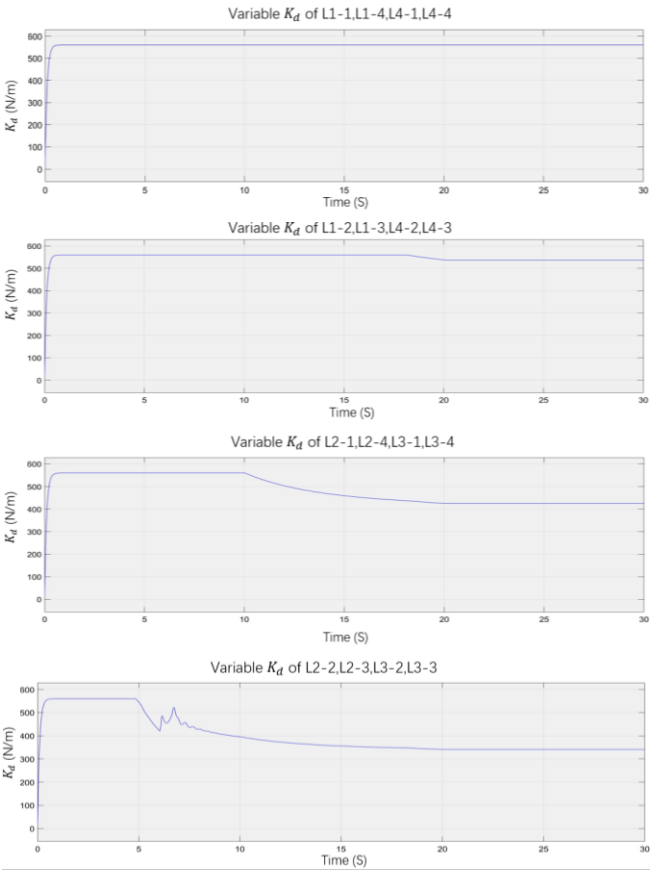

Figure 10. Variable K_d of different pins with respect to time

Because the ball is dropped above the centroid of the shape display, the plots of values of K_d with respect to time of symmetrical pins are the same. The variable K_ds of pins around the corners (L1-1, L1-4, L4-1, L4-4) of the shape display are quite similar, they climb from the minimum (11.76N/m) of K_d's boundary up to maximum (560N/m) and then stay at the maximum boundary. However, the variable K_ds of pins around the centroid of the shape display have been

adjusting themselves from the maximum boundary since different time step. The pins L1-2, L1-3, L4-2 and L4-3 adjust their stiffness from 560.0 N/m at 18.10s to 537.0N/m at 20.25s. The pins L2-1, L2-4, L3-1 and L3-4 adjust their stiffness form 560 N/m at 9.99s to 424.5N/m at 20.36s. The pins L2-2, L2-3, L3-2 and L3-3 adjust their stiffness form 560 N/m at 4.89s, their stiffness oscillate from 4.89s to 8.75s and later decrease gradually to 341.0N/m at 20.19s. The above finding reveals that the decrease of standard deviation of force is mainly due to the adjustments of variable K_ds of pins around the centroid of the shape display.

The force distribution of variable stiffness control at final state is shown in Figure 11.

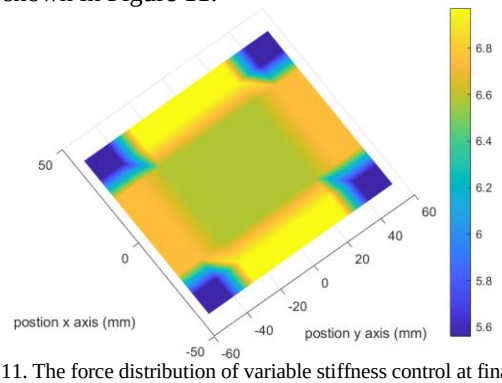

Figure 11. The force distribution of variable stiffness control at final state

The serial number of pins are the same as Figure 8. The maximum of contact force is 6.97N at L1-2, L1-3, L4-2 and L4-3, while the minimum of contact force is 5.60N at L1-1, L1-4, L4-1 and L4-4. The contact force is quite uniform apart from the contact force on four corners.

The maximum of contact force is 6.72N at L1-2,L1-3,L4-2 and L4-3, while the minimum of contact force is 5.98N at L1-1,L1-4,L4-1 and L4-4. The contact force is quite uniform apart from the contact force on four corners. That is because of the limitation of the resolution, pins at four corners can not contact with the ball sufficiently.

To compare the effectiveness of making force distribution evenly between this variable stiffness control and fixed one, different K_ds are chosen as the stiffness parameters for fixed stiffness control. Other conditions such as the weight of the ball are set to be the same as the variable stiffness control. Simulation results of fixed stiffness control are briefly summarized in the Table I.

TABLE I. SIMULATION RESULTS OF FIXED STIFFNESS CONTROL

K_d (N/m)	Peak of standard force deviation(N)	The time cost(s) of the standard deviation to steady state	Magnitude of standard force deviation at steady state(N)
100	17.01	17.72	7.92
200	17.40	(Reaching maximum stroke)	
300	13.50	15.44	1.10
400	12.58	14.52	1.30
500	12.43	15.00	4.58

The standard deviations of force with respect to time of fixed stiffness control with different K_ds are shown in the Figure 12.

When $K_d = 100N/m$, some of the pins such as L2-2, have bottomed up or reached its maximum stroke due to the K_d is too small for the force applied on these pins. Because of this bottom-up phenomenon, there is a bump in the figure of standard deviation of force of fixed stiffness control with $K_d = 100N/m$ at the time of 17s. The bottom-up also happens when $K_d = 200N/m$, and the standard deviation of force oscillates from 21.237s. When $K_d = 300N/m$ or $K_d = 400N/m$, the peak of standard force deviation, the time cost of the standard deviation to steady state and magnitude of standard force deviation at steady state are all smaller than before.

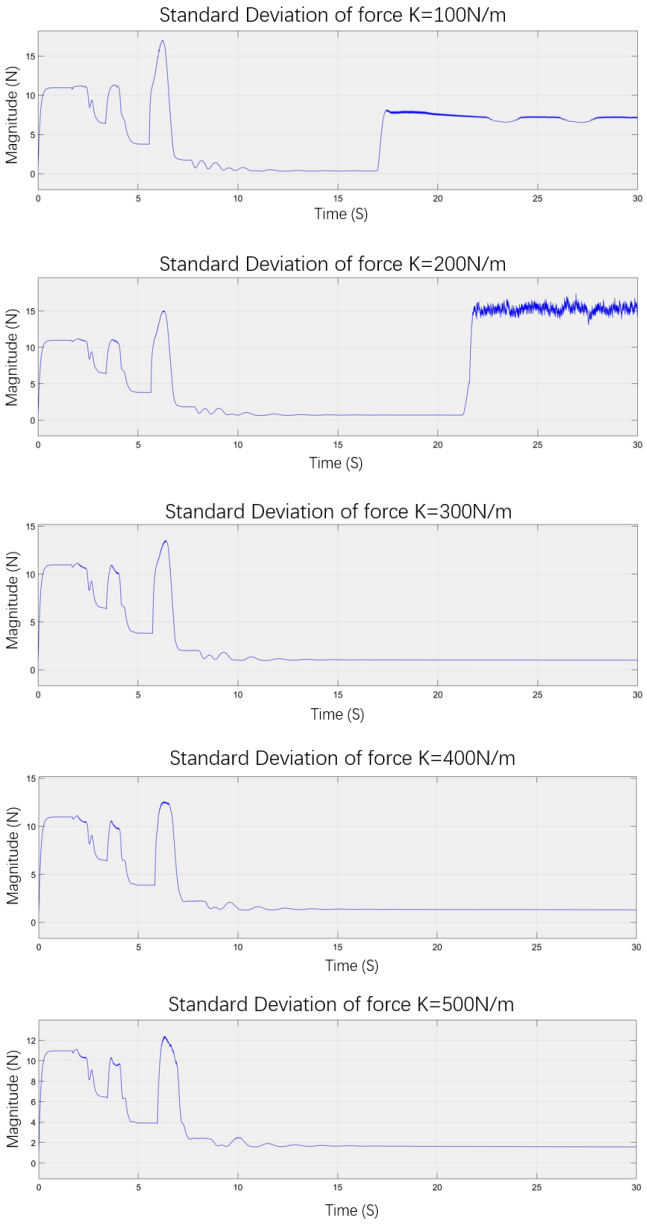

Figure 12. The standard deviation of force with respect to time of fixed stiffness control

The above fixed K_ds applied on the shape display can not out performe the variable stiffness control applied on the shape

display in terms of making the force distribution close to an even state as quickly as possible. Also final state of force distribution of the variale stiffness control is more even compared with fixed stifness ones.

B. Limitations of the simulation

First of all, the parameters of PID controller inside the variable stiffness regulator haven't been fine-tuned and as a result the performance of this control scheme is not fully optimized.

The ball is dropped freely above the centroid of the shape display rather than above corners, and the distance between the surface of the display and centroid of the ball is small, which means start positions of the ball are in a relatively ideal condition. The ball is dropped freely above the shape display rather than conducting certain motions actively, which means the contact between the ball and shape display is not highly dynamical. The performance of this control scheme under highly dynamical condition is not guaranteed.

The ball is only tested with one weight, the shape display hasn't gone through simulation with balls of different weights. what's more, objects of other shapes haven't been tested as well. Therefore, further research needs to be done on improvement of simulation of variable stiffness control.

IV. PROTOTYPE OF 4-BY-4 PIN-BASED SHAPE DISPLAY

In this section a 4-by-4 module will be constructed for demonstration and each pin will be applied with admittance control. The arrangement of pins is shown in Figure 13, distances between each pin are 20.5mm in x direction and 27.5mm in y direction. This module contains 16 pins meaning 4 pins per row with total of 4 rows. The top surface of pin is rectangular of 22mm by 17mm with travel of 25mm.

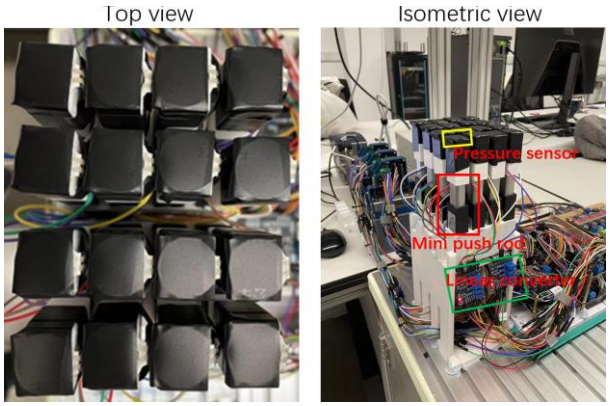

Figure 13. Arrangement of pins

The general setup of this prototype is shown in Figure 14. For each axis of pin (mini push rod with encoder 25mm; LUILEC Ltd., China), the maximum travel is 25mm and the maximum speed is 8mm/s. On top of each pin is a thin film pressure sensor (FSR 18 mm; WAAAX Ltd., China) which enables measurement of force applied on top of each axis. Also, there are 4 linear voltage converters (FSR; WAAAX Ltd., China) converting force signals into analog signals and sending them to the NI CRIO (NI CRIO-9049, C9403 5V/TTL, C9202 ±10V 24bit, National Instrument Automation Inc., USA).

There are also 8 drivers (AT8236, YAHBOOMROBOT Ltd., China) to drive all 16 axis and serve as power supply for film pressure sensors. The readouts of pressure are received by NI CRIO which will be used for calculation of desired position. The NI CRIO servers as the controller of the module and sends out control signals, embedded FPGA enables it to control each axis simultaneously. A USB cable connects both the PC and NI CRIO. The PC serves as a user interface on which the user can specify the stiffness and damping of each axis. The software is using the labview19.0.

First, the force sensor senses the external force applied on the top of the pin. The force signal is converted into analog signal via the linear converter. And then this analog signal is sent to the CRIO and received by the NI9202 module plugged on the CRIO chassis. Later, CRIO calculates the desired position of pin and the desire speed of the pin. The result is that the CRIO will send the PWM signal of certain duty via NI9403 module.

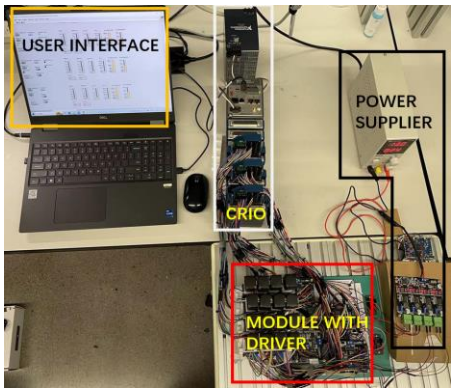

Figure 14. General setup of 4-by-4 pin-based shape display

The PWM signal will determine how much power to be drawn from the power supplier via motor driver or in a more intuitive way, the linear velocity of pin. The pin will stop accordingly as it has arrived at desired position. A series of experiments will be conducted in next chapter for performance evaluation of the device.

V. EXPERIMENTATION AND RESULTS

The tested parameters have to be chosen according to the specification of both the sensor and the motor. The sensor can measure force of 0.294N up to 14N and the magnitude analog signal of force sensor (0-3.3V) is roughly proportional to the force magnitude. The motor travel is 25mm and the maximum speed of motor is 8mm/s. These parameters will be helpful in terms of choosing the range of stiffness and damping.

$$K_{max} = \frac{F_{max}}{d} = \frac{14N}{0.025m} = 560N/m \quad (18)$$

$$K_{min} = \frac{F_{min}}{d} = \frac{0.294N}{0.025m} = 11.76N/m \quad (19)$$

$$D_{min} = \frac{F_{min}}{V_{max}} = 3.65Ns/m \quad (20)$$

A. Experiment I: Evaluation of dynamical performance of shape display.

In this experiment a weight of 500g was dropped freely from a position close to the top of pin when the pin was

extended fully. Three different stiffness value were chosen randomly. The displacement with respect to time was recorded for the comparison between real performance and the simulated one. The set up of the experiment is shown in the Figure 15.

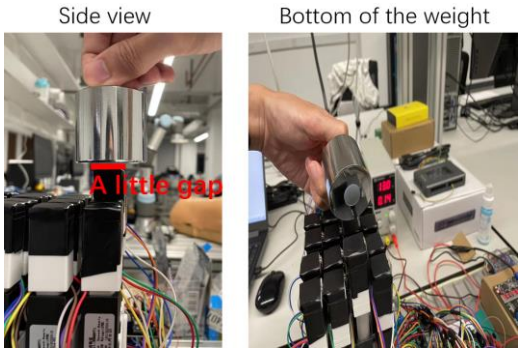

Figure 15. Setup of single pin evaluation

For each different stiffness, 10 trials were recorded per pin and all 16 pins were under evaluation. The average of recorded data and the standard deviation at each time step are shown in the Figure 16.

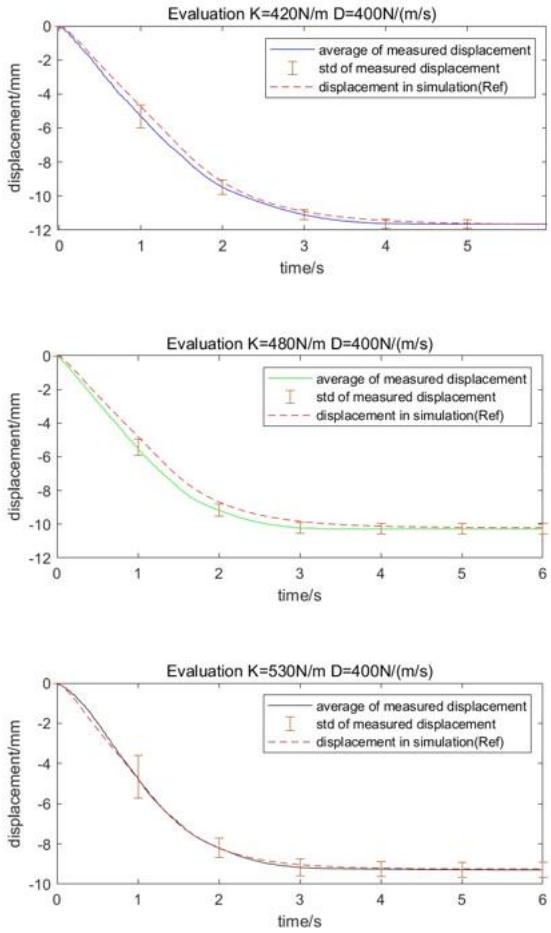

Figure 16. Simulated displacement vs average of measured displacement. The error bars represent the standard deviation values at 0s,1s,2s,3s,4s,5s and 6s. The setup with K=530N/m and D=400Ns/m at 1s has the maximum standard deviation of 1.0741mm. The setup with K=420N/m and D=400Ns/m at 4s has the minimum standard deviation of 0.2600mm.

The average standard deviation for three setups from top to bottom in figure 16 are 0.3673mm, 0.3473mm and 0.5132 correspondingly. The average of measured displacement of different stiffness generally follows the simulated result. To achieve higher accuracy more advanced hardware as well as improvement in existing control scheme are needed[13]. And the goals of achieving better accuracy as well as making the system more robust will also be included in future work.

B. Experiment II: Subjective evaluation of shape display.

In this experiment, the module was assessed based on the subjective experience of the experimenter. There was one of the five different stiffness parameters, namely, 50N/m, 100N/m, 200N/m, 300N/m, 400N/m combined with two different damping parameters, namely, 3.65Ns/m and 3.65Ns/m. Each combination comprised ten trials total of 100 trials per experimenter. The resistance felt while pushing down the single pin was rated in a scale of one to ten. The results of the subjective evaluation for a single pin recorded are in the Table II.

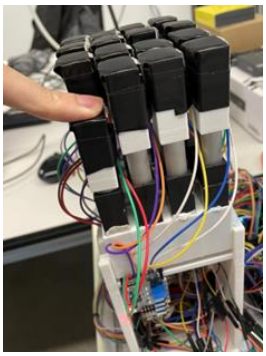

Figure 17. Subjective experiment of each pin

TABLE II. SCORES OF EFFORT TO PUSH DOWN THE PIN

Stiffness(N/m)	***Damping(N/(m/s))***	***Average Scores***
50	3.65	1.5
100		2.4
200		3.5
300		4.4
400		5.4
50	1000	6.1
100		7.2
200		8.4
300		9.1
400		9.7

The experimenter reported that interacting with the module with the palm was more comfortable than interacting with one finger.

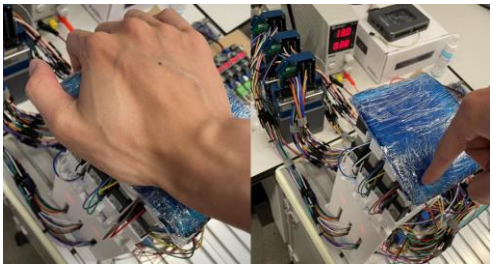

Figure 18. Left: Interaction with palm,Right:Interaction with finger

There were oscillations when damping parameter was small. As the damping parameter increasing or the pins were pushed deeper down oscillations would not occur. These issues can also be improved by increasing the sampling rate of force sensing. The above objective assessments only revealed some plain facts. In the future, we may also look into some insights such as finding the balance between the safety and the accuracy of mimicking a real spring-damper for the future improvements.

VI. Discussion

As demonstrated in the experiments, our device can be used to render surface of different stiffness and damping. For example, when a certain type of material is under development, the data of stiffness is not intuitive and using other materials as approximations is not accurate. In this scenario, our device can mimic the elastic and viscous elastic properties of the material for intuitive sensation helpful in the material specification and selection process. Another application is in the rendering of not just the geometry but also the dynamics and haptics in virtual reality.

However, there are some limitations. First, although the stiffness and damping of each pin can be specified individually, both of them have to be set manually. Variable stiffness control is only evaluated in simulation not in reality. Although the accuracy of position control and velocity error have been evaluated in some form of quantified ways. The objective tests involved with experimenter have only revealed some obvious facts not useful insights. The device and its control scheme have to prove themselves in more rigorous users' tests.

Just like all the pin-based shape display this module has its limitation of rendering resolution. However, depending on different using scenarios the resolution is not the higher the better.

VII. Conclusion

Admittance control is applied in this research and a variable stiffness control is proposed as well. The real module can behave compliantly with human hands as well as other objects. The proposed variable stiffness control is more stable than the fixed one and the force distribution and the force distribution is more even. The variable stiffness control converges faster into the steady state. The real module achieves expected properties under the subjective evaluations and expected performance under objective evaluation.

Realization of a bigger scale module with higher resolution and more refined control scheme are goals of technical improvements we want to pursue. The long-term goal in general is that we want to make the module into a kind of application in everyday life, for example a novel pillow for better sleeping quality. There is still a long way to go.

References

[1] M. Coelho and J. Zigelbaum, "Shape-changing interfaces," *Personal and Ubiquitous Computing*, vol. 15, no. 2, pp. 161-173, 2011/02/01 2011.

[2] H. Iwata, H. Yano, F. Nakaizumi, and R. Kawamura, "Project FEELEX: Adding haptic surface to graphics," (in English), *Siggraph 2001 Conference Proceedings*, pp. 469-475, 2001.

[3] M. Feick, N. Kleer, A. Zenner, A. Tang, and A. J. P. o. t. C. C. o. H. F. i. C. S. Krüger, "Visuo-haptic Illusions for Linear Translation and Stretching using Physical Proxies in Virtual Reality," 2021.

[4] A. F. Siu, E. J. Gonzalez, S. Yuan, J. B. Ginsberg, and S. Follmer, "shapeShift," presented at the Proceedings of the 2018 CHI Conference on Human Factors in Computing Systems, 2018.

[5] S. Follmer, D. Leithinger, A. Olwal, A. Hogge, and H. Ishii, "inFORM," presented at the Proceedings of the 26th annual ACM symposium on User interface software and technology, 2013.

[6] N. Ken, L. Yingda, N.-A. Chloe, and H. Ishii, "TRANS-DOCK: Expanding the Interactivity of Pin-based Shape Displays by Docking Mechanical Transducers," *Proceedings of the Fourteenth International Conference on Tangible, Embedded, and Embodied Interaction*, vol. null, p. null, 2020.

[7] S. Pedro de Almeida, R. Ferreira, and M. Andrade, "Bezalel - Towards low-cost pin-based shape displays," *SIGGRAPH Asia 2019 Technical Briefs*, vol. null, p. null, 2019.

[8] R. Suzuki, N. Ryosuke, L. Dan, Y. Kakehi, M. Gross, and L. Daniel, "LiftTiles," *Proceedings of the Fourteenth International Conference on Tangible, Embedded, and Embodied Interaction*, vol. null, p. null, 2019.

[9] K. Nakagaki, D. Fitzgerald, Z. Ma, L. Vink, D. Levine, and H. Ishii, "inFORCE: Bi-directional `Force' Shape Display for Haptic Interaction," presented at the Proceedings of the Thirteenth International Conference on Tangible, Embedded, and Embodied Interaction, Tempe, Arizona, USA, 2019.

[10] M. Schumacher, J. Wojtusch, P. Beckerle, and O. von Stryk, "An introductory review of active compliant control," *Robotics and Autonomous Systems*, vol. 119, pp. 185-200, 2019/09/01/ 2019.

[11] C. Ott, R. Mukherjee, and Y. Nakamura, "Unified Impedance and Admittance Control," in *2010 IEEE International Conference on Robotics and Automation*, 2010, pp. 554-561.

[12] A. Lecours, B. Mayer-St-Onge, and C. Gosselin, "Variable admittance control of a four-degree-of-freedom intelligent assist device," in *2012 IEEE International Conference on Robotics and Automation*, 2012, pp. 3903-3908.

[13] O. Shoon So, N. H. H. M. Hanif, and I. Elamvazuthi, "Closed-loop force control for haptic simulation: Sensory mode interaction," in *2009 Innovative Technologies in Intelligent Systems and Industrial Applications*, 2009, pp. 96-100.